



ANALYSIS OF HEAT RECOVERY IN GAS–SOLID MOVING BEDS USING A SIMULATION APPROACH

A. C. Caputo, G. Cardarelli and P. M. Pelagagge*

Department of Energetics, Faculty of Engineering, University of L'Aquila, 67040 Monteluco, L'Aquila, Italy

(Received 5 December 1994)

Abstract—This work represents a first contribution to a research programme directed towards the optimization of heat recovery from moving beds running under unsteady-state conditions. A simulation model able to represent the gas–solid bed behaviour for different operating parameters and design choices has been presented. The approach has been detailed with reference to the air-cooled bed of a sintering plant for blast furnace feeding. The sintering cooler of the Taranto Ilva steel plant, in particular, has been examined. The results of the model provide useful indications for the design and management of the heat recovery system.

Keywords—Heat transfer, moving (packed) bed, heat recovery, iron-ore sintering, computer simulation.

NOMENCLATURE

A	cell heat transfer surface [m ²]
A_c	computation cell cross-sectional area [m ²]
C	heat capacity [W/K]
d	mean particle diameter [m]
F	flow rate [kg/s]
h	convective heat transfer coefficient [W/m ² K]
K	air thermal conductivity [W/m K]
L	hood length [m]
Pr	Prandtl number
Re	Reynolds number
Q	heat flow exchanged in computation cell [J/s]
T	temperature [°C]
V_c	computation cell volume [m ³]

Greek symbols

ϵ	void fraction
μ	air viscosity [N s/m ²]
ϕ	shape factor

Subscripts

A	air
S	sinter
f	fresh air
i	inlet
o	outlet
1	first hood
2	second hood

1. INTRODUCTION

The design of heat recovery systems is strongly affected by the trends of the thermal characteristics of the source to be exploited. These trends first of all influence the choice of the thermal consumer and, consequently, the definition of the recovery ratio.

In the case of gas–liquid streams, a direct heat transfer is usually possible, allowing for an explicit correlation between the thermal characteristics of the source and the consumer. The design choices generally involve the optimal synthesis of the heat exchanger network [1, 2].

*Author to whom correspondence should be addressed.

In the case of solid moving beds, a transfer fluid connecting the source to the consumer has often been necessary. The heat recovery system may then be subdivided into two sections: one dedicated to the heat exchange between the solid bed and the transfer fluid, the other to the transfer of the recovered heat to the consumer.

The aim of this work is the development of a simulation tool able to represent the thermal behaviour of the first section. Mathematical models based on different degrees of accuracy in solid bed schematizing may be found in the literature [3–10]. Moreover, the packed bed cooling process has sometimes been approximated to the behaviour of a thermal storage unit undergoing single-blow operation [11–15]. As far as the evaluation of heat transfer parameters is concerned, a vast body of literature is available too. Simplified approaches, both of experimental or theoretical-semi-empirical types, normally refer to beds with identical particles of the same shape [16–21]. Spherical particles are frequently assumed in theoretical models [22, 23].

More sophisticated approaches take into account both:

- (a) the interaction of gas–solid convection and conduction both inside and among the particles [24–27];
- (b) the geometrical and the fluid flow complexities [27].

For the purposes of this research, orientated towards the optimization of the heat recovery system, an accurate rating of the average gas temperature produced from the solid bed only proves necessary. Such a result has been pursued describing the bed as a matrix of cross-flow heat exchangers and adopting a generalized correlation for the convective heat transfer coefficient evaluation.

In this way a simplified simulation model has been developed that is able to take into account the particle granulometry effects, but not the conduction ones. As a reference scenario for the study, the air-cooled bed of a sintering plant for blast furnace feeding has been assumed. The sintering cooler of the Taranto Ilva steel plant, in particular, has been considered as a reference point for the simulation results.

The agreement of the calculated data with the experimental ones, but also with the results of a more detailed schematization [27], demonstrates the effectiveness and generality of the proposed simulation approach.

2. REFERENCE SINTERING PLANT

The solid bed taken as the reference scenario for the study is represented by the cooling section of a sintering plant for blast furnace feeding. The sintering plant (Fig. 1) consists essentially of two moving beds: the sintering bed and the cooling bed. A mixture of iron ore, coke breeze and some additives is used as feed raw material for the sintering bed. The ignition furnace brings about the combustion of the upper layers of the raw material. The combustion propagates towards the underlying layers until the bottom of the sintering bed is reached. A cooling of the upper layers of the bed obviously occurs due to the air flow used to support combustion.

The sintered material at the end of the bed appears as a continuous, porous and permeable solid with very different temperatures among the layers. When the sinter falls on the cooling bed, clods of different shapes and granulometry are obtained. Larger particles compared to other plants [27, 28] have been produced at the Ilva sinter bed, with a size distribution ranging from 0 to 300 mm

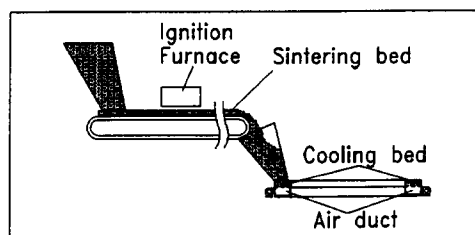


Fig. 1. Sintering plant.

and an average value of 100 mm. The void fraction of the cooling bed has been estimated to be 0.4, having assumed a porous material density of 2700 kg/m^3 and measuring a bulk density of 1600 kg/m^3 .

A rotary breaker facilitates the sinter crushing, also mixing the clods at different temperatures. As a consequence, only an average temperature of the sinter at the inlet of the cooling bed may be defined. This value varies from 500 to 600°C depending on the running condition of the sintering bed. The sinter flow rate varies instead from 110 to 180 kg/s . The final temperature of the sinter has to be about 60°C .

The cooling bed consists of a continuous series of 50 bottom-gate trolleys moving along a ring in a circular duct. Six fans are linked to the duct, each one able to process 140 kg/s of air. The ring has an average radius of 20 m and a width of 4 m . A constant cooling bed height of about 0.8 m is maintained, adjusting the moving velocity in order to follow the sinter flow rate variations. The working length of the cooling zone is about 100 m , normally requiring a holding time of 3000 – 5000 s .

3. HEAT RECOVERY PROBLEM STATEMENT

The heat recovery from a cooling bed obviously requires air collection by means of one or more hoods. The consumer's choice depends on the minimum temperatures of the air streams that may be collected. Such temperatures and the relative air heat contents are evidently linked to:

- (a) the operating parameters at the inlet of the cooling bed (sinter temperature and flow rate, air temperature and flow rate);
- (b) the lengths and positions of the hoods.

Considering only a steady-state running condition it is possible to unequivocally correlate the air outlet temperature and flow rate within the length of the hoods. The cooling bed operating condition is not actually of the steady-state type, due to various reasons:

- (a) the *sinter inlet flow rate* (F_{Si}) may vary, depending on the sintering bed flow rate fluctuations linked to production requirements, and on the frequent maintenance stops which introduce restart transients;
- (b) the *sinter inlet temperature* (T_{Si}) may vary, depending on the sintering bed height and velocity, and on the temperature and humidity of the combustion air;
- (c) the *air inlet temperature* (T_{Ai}) may vary, depending on the weather situation;
- (d) the *air inlet flow rate* (F_{Ai}) may vary, depending on its use as an adjusting parameter to guarantee sufficient cooling of the sinter.

It may be pointed out that while the T_{Si} and F_{Si} values are imposed from the sinter machine process condition, the T_{Ai} and F_{Ai} values may be further varied to optimize the heat recovery process.

The sinter cooling must evidently be assured, but considering that the cooling bed is normally designed for the peak operating condition (maximum T_{Si} , F_{Si} and T_{Ai} values), solutions leading towards an increase of the collected air temperature may be pursued. In particular, the feeding of a cooling bed section with higher air temperature may be implemented.

These configurations appear particularly appropriate in the productive scenario examined, considering the little interest in low temperature heat recovery.

Different solutions have been conceived for the waste heat recovery from sintering plants [28–31]; however, the optimum one has not yet been defined. The aim of this research is the development of an optimization methodology for the design and management parameters for heat recovery systems from unsteady-state solid beds. The study refers to the recovery scheme shown in Fig. 2, which allows for a representation of the main plant solutions. In particular, the following solutions have been considered:

- (a) just one type of consumer fed by:
 - one hood (case a),
 - one shutterable hood (case b),
 - two series hoods (case c);

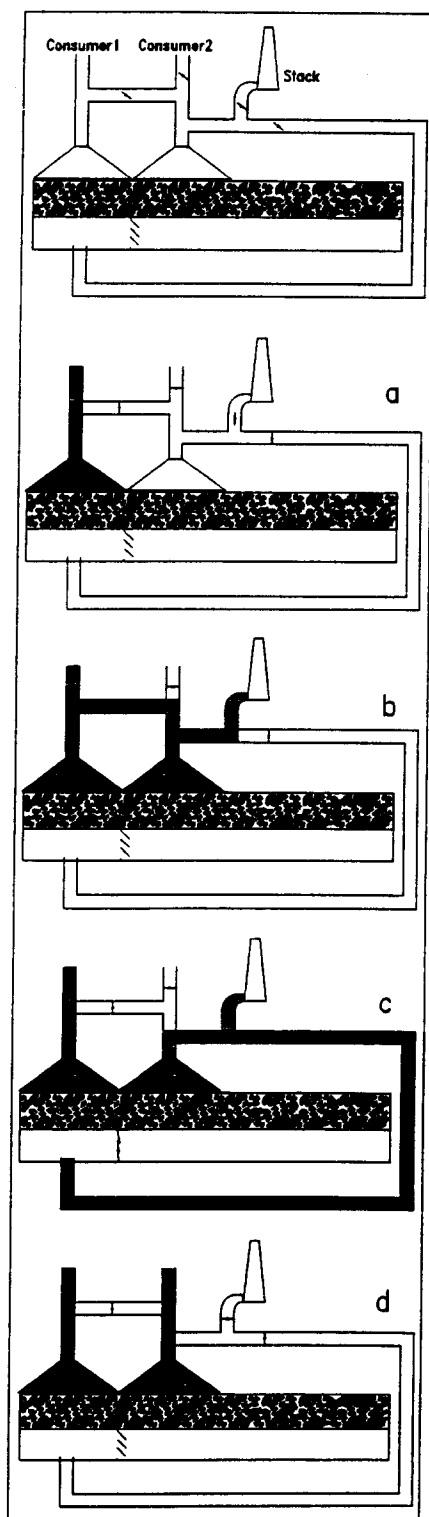


Fig. 2. Heat recovery scheme.

- (b) two or more consumer types fed by:
 —two or more parallel hoods (case d).

The hood lengths represent, in all cases, one of the design parameters to be optimized. This paper deals with a simulation approach able to describe the cooling bed behaviour for different design choices and operating conditions.

4. COOLING BED SIMULATION

4.1. Simulation approach

The cooling bed has been schematized as a matrix of cross-flow heat exchangers. Different numbers of rows and columns of the matrix scheme may be considered by the simulation model.

At the outlet of each matrix cell the gas and the solid temperatures have been respectively expressed using the obvious heat balances:

$$T_{Ao} = T_{Ai} + \frac{Q}{C_A} \quad (1)$$

and

$$T_{So} = T_{Si} - \frac{Q}{C_s}, \quad (2)$$

where C represents the heat capacity of each stream.

Equations (1) and (2) may be directly solved using, for the heat flow exchanged (Q) in each computation cell, a formulation hypothesizing a logarithmic mean temperature difference:

$$Q = (T_{Si} - T_{Ai}) \frac{1 - q}{1/C_A - q/C_s},$$

where $q = \exp[hA(C_A - C_s)/C_A C_s]$.

The specific heat for the sinter has been assumed as equal to 920 J/kg K.

The convective heat transfer coefficient between particles and fluid has been evaluated by [32]:

$$h = \frac{K}{\epsilon d} (2 + 0.75 \text{Pr}^{0.33} \text{Re}^{0.5}).$$

A Reynolds number based on the particle diameter has been adopted:

$$\text{Re} = \frac{F_{Ai} d}{\mu A_c}.$$

At each calculation step the thermophysical properties of flowing gas have been reevaluated according to the average local temperature.

The particle diameter at each cell has been defined by resorting to a stochastic function with an average value equal to 100 μm .

An average value of the void fraction for all the bed has been adopted ($\epsilon = 0.4$). The heat transfer surface may be evaluated for each matrix cell by:

$$A = 6 \frac{1 - \epsilon}{d} V_c \phi,$$

where ϕ represents a shape factor defined as the ratio between specific surfaces of the sinter particles and the equivalent diameter spheres. Few data are available for the sinter shape factors, a range from 1 to 1.7 has been proposed [27, 32, 33]. A value of 1.6 has been adopted for the Ilva sinter particles.

The initial distribution of the solid temperature has been assumed to be uniform. Different initial values for the air flow rate and temperature may instead be supplied along the bed.

4.2. Model verification

The solution stability has been preliminarily verified when the number of matrix cells were changed. A high robustness characterizes the discretization scheme; by varying the matrix cell number from 100 to 2000, air temperature and sinter temperature variations always less than 5%

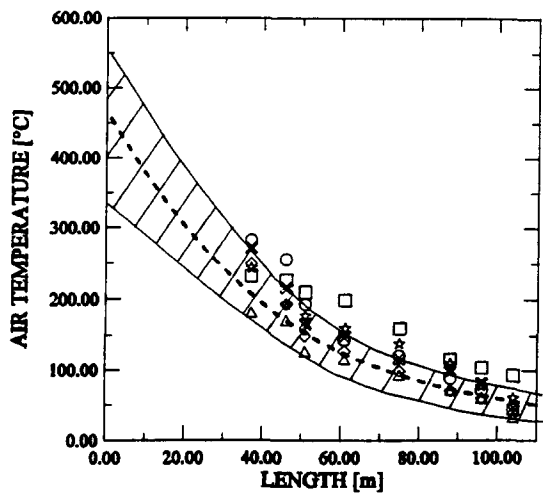


Fig. 3. Local air temperature comparison.

have been observed. The effectiveness of the simulation model has then been verified with reference to the two typologies of experimental data available for the cooling bed of the Ilva sintering plant.

The first set of experimental data refers to local air temperature measurements. Sensors were allocated in different sections of the bed, between 30 and 100 m. Temperature sensors cannot be allocated in the first 30 m of the bed due to access reasons.

Six series of surveys for each measure point have been available (Fig. 3). The experimental data scattering may be ascribed both to the difficulty in strictly controlling the operating conditions and to the flow channelling phenomena. The simulation has been performed considering an average set of operating conditions, close to the one which occurs more frequently (Table 1). The other simulation input data are as previously defined. The hatched region in Fig. 3 represents the effect of the particle size stochastic distribution, the dashed line instead shows the simulation result considering the average particle diameter. The accuracy in describing the local air temperature appears satisfactory, especially when the wide operating condition variability of the actual cooling bed has been taken into account.

Only the simulation results referring to the average particle diameter will be presented in the following analyses.

A second set of experimental data refers to the average air temperature collected over the first 28 m of the bed. The measurements have been available for different air inlet temperatures (T_{Ai}), ranging from 80 to 130°C (Fig. 4). The other operating conditions have been assumed as in Table 1. The line of Fig. 4 shows the results obtained with the simulation model running under the same experimental operating conditions.

The agreement of the simulation results along the bed length with both the local air temperature and the average air temperature appears compatible with the aims of this study. In order to verify the model capability in describing different cooling beds, and in particular the generality of the correlation adopted for the heat transfer coefficient, a comparison with the results obtained in Ref. [27] has been carried out. Table 2 shows the characteristics and the operating conditions of the sinter cooler examined in that study. In Ref. [27] the heat exchange performances were evaluated using a two-dimensional random-packed model able to take into account the effects of solid conduction, air flow distribution, size segregation and initial sinter temperature distribution. The air temperature change at the bed outlet calculated in Ref. [27] is shown by the hatched region in Fig. 5.

Table 1. Average operating conditions

F_{Si} [kg/s]	T_{Si} [°C]	F_{Ai} [kg/s]	T_{Ai} [°C]
155	550	450	20

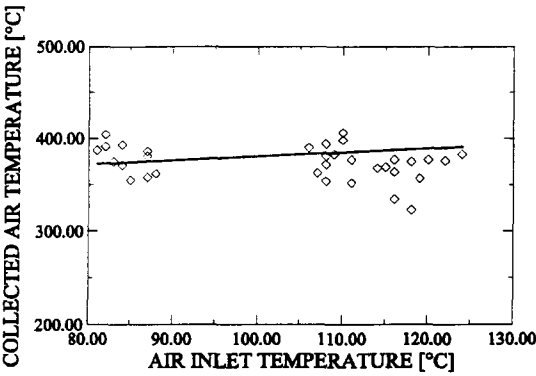


Fig. 4. Average air temperature comparison.

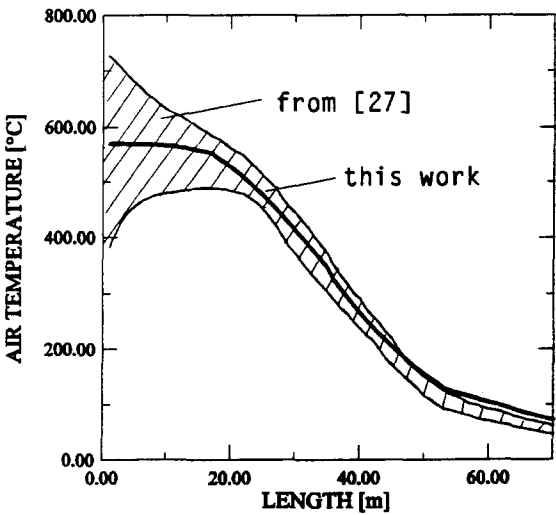


Fig. 5. Comparison with results from Ref. [27].

The simulation result obtained in this work is indicated by a single line on the figure. The result’s agreement with a very detailed model supports the generality of the proposed approach.

4.3. Analysis results

Considering the wide variability of the operating conditions typical of a sinter cooler, and in particular of the reference one, an analysis has been carried out in order to point out the effects of the sinter inlet thermal flow rate and of the air inlet temperature on the recoverable heat and collected air temperature.

Effect of the sinter inlet thermal flow rate. Figure 6 shows the effect of the sinter inlet temperature. A variability range from 500 to 600°C has been examined. The figure shows the trends of the air outlet temperature along the cooling bed length. Furthermore, the recoverable heat and the corresponding average temperature of the collected air have been evaluated, hypothesizing different hood lengths. An increase of the sinter inlet temperature naturally allows for both an increase of the recovered heat and of the air temperature. A similar effect has been displayed from the mass flow rate of the sinter (Fig. 7). A variability range from 116 to 183 kg/s has been examined. A greater sensitivity with respect to this parameter, both of the air temperature and of the recovered heat, has been observed, as pointed out in the figure.

Combining both effects, the trends shown in Fig. 8 have been obtained. In all cases an air inlet temperature equal to 20°C and a constant air flow rate equal to 450 kg/s have been considered for comparison reasons. The sinter cooling obtained as a simulation result satisfies the process requirements.

Effect of the air inlet temperature. Figure 9 shows the results obtained considering that preheated air has been fed underneath the entire cooling bed. Two different air inlet temperatures have been considered: 80 and 150°C, respectively. The air flow rate has been increased up to 720 kg/s, in order to reduce the sinter outlet temperature. The values of Table 1 are assumed for the sinter initial conditions. As a result, an increase of the recovered heat and of the collected air temperature has been observed, above all in the case with $T_{Ai} = 150^{\circ}\text{C}$.

Table 2. Cooling bed characteristics from Ref. [27]

Bed		Operating conditions	
Length:	70 m	F_{Si} :	230 kg/s
Width:	4 m	T_{Si} :	570 °C
Height:	1.75 m	T_{Ai} :	20 °C
Holding time:	2400 s	$F_{Ai} < 17.5$ m:	63.7 kg/s
d :	9.7 mm	from 17.5 to 35 m:	97.4 kg/s
ϕ :	1	from 35 to 52.5 m:	120 kg/s
ϵ :	0.4	from 52.5 to 70 m:	79.5 kg/s

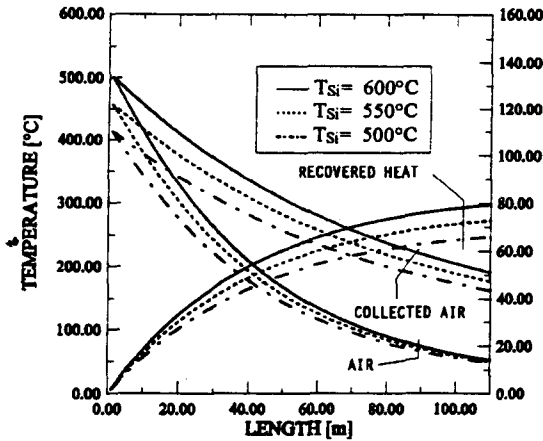


Fig. 6. Effect of the sinter inlet temperature.

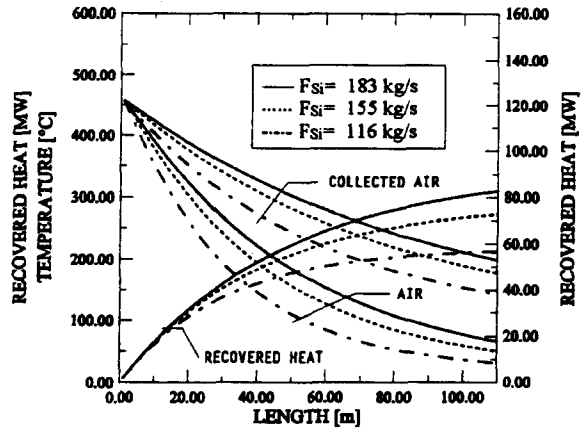


Fig. 7. Effect of the sinter mass flow rate.

In this way, preliminary indications on the recoverable heat may be obtained, without, however, taking into account the sinter cooling temperature. Such a temperature result is, in fact, not completely suitable for the process requirements, as shown in Fig. 9(a).

A proper sinter cooling, at the same time improving the heat recovery performances, may be obtained by feeding preheated air under a first bed section only (first hood) and fresh air along the remaining bed length (second hood). The simulation results considering three different lengths of the first hood are shown in Fig. 10, for $T_{Ai1} = 150^{\circ}\text{C}$ and $T_{Ai2} = 20^{\circ}\text{C}$.

The second hood may be used to produce the preheated air. Establishing by an air preheating level required for the first hood, this constraint may be satisfied using two hoods of the same length under only one condition, in the case of $T_{Ai1} = 150^{\circ}\text{C}$ [Fig. 10(b)]; that is: $L_1 = L_2 = L_c/2$.

For every first hood length ($L_1 < L_c/2$) there may be unequivocally defined a second hood length ($L_2 < L_1$) that produces a specific preheated air flow rate. This preheated air has to be mixed with fresh air, in order to obtain the flow rate required by the first hood, respecting also the temperature constraint.

Generally speaking, the problem may be formulated as:

searching for L_2 able to collect an air flow that, after a mixing with fresh air, satisfies the first hood requirements in terms of both flow rate and temperature.

These kinds of problems may be quickly solved by using the simulation model. An example solution that assumes a 150°C preheating level required by the first hood is illustrated in Fig. 11. The second hood length (L_2), the relative collected air temperature (T_{Ao2}) and the mixing fresh air flow rate (F_r) are shown for different first hood lengths.

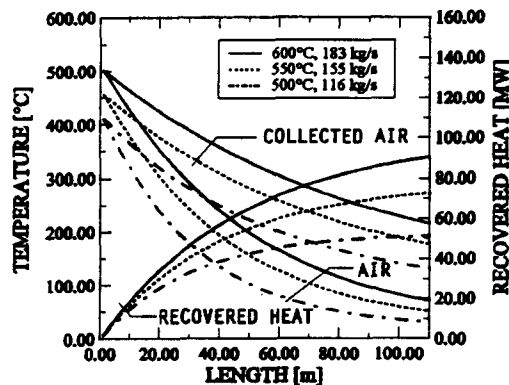


Fig. 8. Effect of the sinter inlet thermal flow.

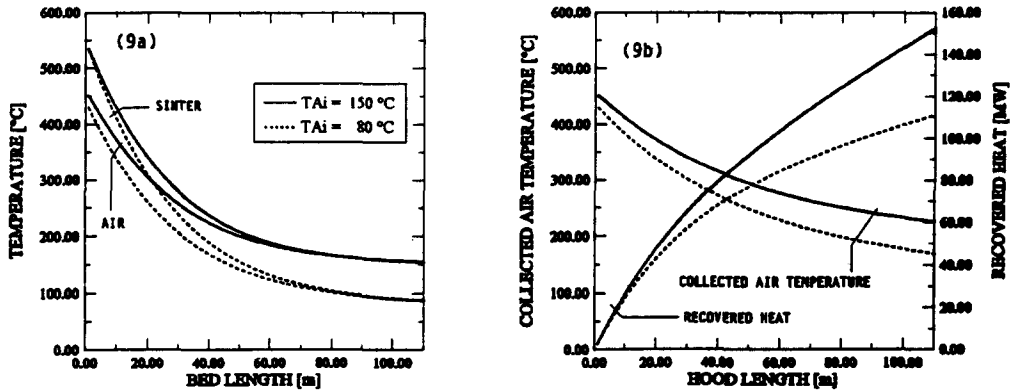


Fig. 9. Effect of the air inlet temperature.

For L_1 greater than $L_c/2$, a second hood length able to satisfy the first hood requirement obviously cannot be found.

It can be finally pointed out that by reducing the preheating at the first hood an increase of the L_c value may be obtained.

5. CONCLUSIONS

The aim of the research program is the development of a methodology for optimizing the heat recovery from moving beds which operate under unsteady-state conditions. In this paper, the thermal behaviour of a sintering cooler bed has been characterized considering different design choices and operating conditions. A simulation model of heat recovery in gas–solid moving beds

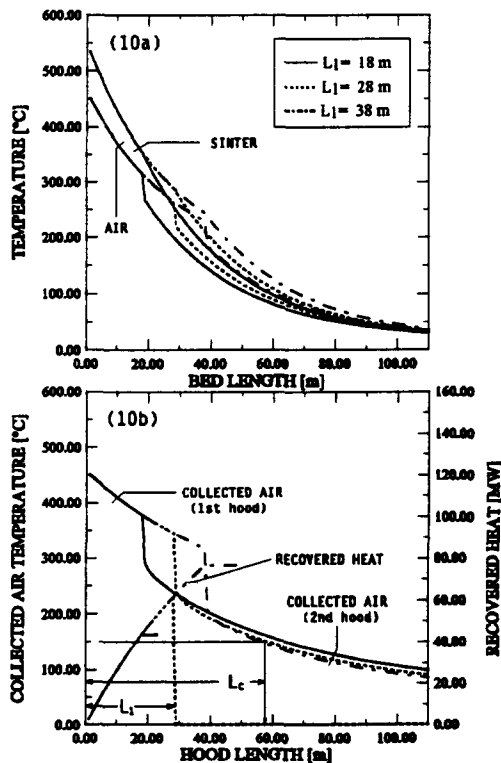


Fig. 10. Effect of the first hood length.

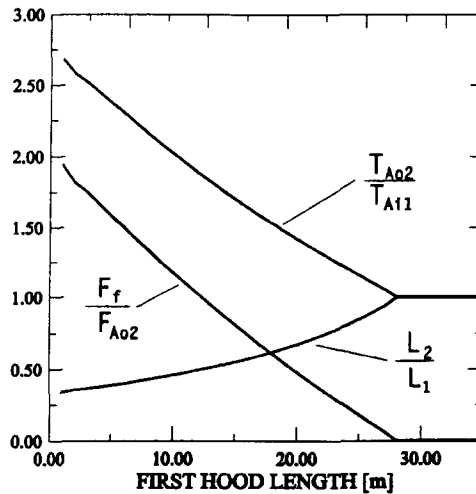


Fig. 11. Two hoods problem solution.

has been developed that provides a sufficient approximation to evaluate the thermal characteristics of the air being produced and the cooling level of the solid phase.

The research progress foresees the implementation of a new model, representing the entire heat recovery plant, and capable of matching the recoverable heat trend to the consumer thermal load trend. In this way, the evaluation of the actual heat recovery and, therefore, the economical benefits that may be reached, will be possible.

REFERENCES

1. Floudas, C. A., Ciric, A. R. and Grossmann, I. E., Automatic synthesis of optimum heat exchanger network configurations. *AIChE J.* **32**(2), 276–290 (1986).
2. Nishida, N., Stephanopoulos, G. and Westerberg, A. W., A review of process synthesis. *AIChE J.* **27**(3), 321–351 (1981).
3. McCoy, B. J. and Maallov, O., Dynamics of heat transfer in packed bed. *Proc. 29th Heat Transfer and Fluid Mechanics Inst.*, Sacramento, CA, 20–21 June 1985, pp. 149–158.
4. Heggs, P. J., *Transient Packed Bed Heat Transfer: Numerical Solutions, Computational Techniques in Heat Transfer*, Vol. 1, pp. 299–329. Pineridge Press.
5. Dixon, A. G. and Cresswell, D. L., Effective heat transfer parameters for packed bed models. *AIChE J.* **32**(5), 809–819 (1986).
6. Baclic, B. S. *et al.*, Differential fluid enthalpy method for predicting heat transfer coefficient in packed beds. *Proc. 8th Int. Heat Transfer Conf.*, San Francisco, CA, 17–22 August 1986, pp. 2617–2622.
7. Hoerger, C. R. B. and Phillips, W. F., Limitations of the single phase model for solid gas heat transfer in packed beds. *ASME J. Heat Transfer* **107**, 260–262 (1985).
8. Amudsen, W. R., Solid fluid interactions in fixed and moving beds. *Ind. Engng Chem.* **48**, 1–50 (1956).
9. Galloway, T. R. and Sage, B. M., A model of the mechanism of transport in packed, distended and fluidized beds. *Chem. Engng Sci.* **25**, 495 (1970).
10. McGaw, D. R., Gas particle heat transfer in a cross-flow moving packed bed heat exchanger. *Powder Technol.* **13**(2), 231–239 (1976).
11. Larsen, F. W., Rapid calculation of temperature in a regenerative heat exchanger having arbitrary initial solid and entering temperatures. *Int. J. Heat Mass Transfer* **10**, 149–168 (1967).
12. Hamilton, N. I., Heat and mass flow analysis of packed bed thermal regenerators. *Massachusetts Inst. of Technol.*, Report 02173, pp. 104–106 (1978).
13. Montakhab, A., Convective heat transfer in porous media. *ASME Heat Transfer* **101**, 507–510 (1979).
14. Beasley, D. E. and Clark, J. A., Transient response of a packed bed for thermal energy storage. *Int. J. Heat Mass Transfer* **27**(9), pp. 1659–1665 (1984).
15. Schmidt, F. W., Single-blow operation. *Heat Exchanger Design Handbook*, Vol. 3, Sec. 15.12, pp. 1–13. VDI, Berlin.
16. Seshadri, V. and Da Silva Pereira, R. O., Comparison of formulae for determining heat transfer coefficient of packed beds. *Trans. Iron and Steel Inst. of Japan* **26**(7), 604–610 (1986).
17. Lemcoff, N. O. *et al.*, Heat transfer in packed beds. *Rev. Chem. Engng* **6**(4), 229–292 (1990).
18. Kunii, D. and Suzuki, M., Particle to fluid heat and mass transfer in packed beds of fine particles. *Int. J. Heat Mass Transfer* **10**, 845–852 (1967).
19. Barker, J. J., Heat transfer in packed beds. *Ind. Engng Chemistry* **57**(4), 43–51 (1965).
20. Crawshaw, J. P. *et al.*, Transport properties in moving packed beds. *3rd UK Conf. on Heat Transfer*, Birmingham, 16–18 September 1992, Vol. 2, pp. 1093–1098.
21. Gnielinski, V., Fixed beds. *Heat Exchanger Design Handbook*, Vol. 2, Sec. 5.4, pp. 1–7. VDI, Berlin (1983).

22. Achenbach, E., Heat and flow characteristics of packed beds. *Proc. 3rd Conf. on Experimental Heat Transfer, Fluid Mechanics and Thermodynamics*, Vol. 1, pp. 283–293 (1993).
23. Malling, C. F. and Thodos, G., Analogy between mass and heat transfer in beds of spheres: contributions due to end effects. *Int. J. Heat Mass Transfer* **10**, 489–498 (1967).
24. Balakrishnan, A. R. and Pei, D. C. T., Heat transfer in fixed bed gas–solid systems. *Chem. Engng Sci.* **30**, 293–300 (1975).
25. Balakrishnan, A. R. and Pei, D. C. T., Heat transfer in gas–solid packed bed systems. *Ind. Engng Chem. Process Des. Dev.* **18**(1), 30–50 (1979).
26. Martinez, O. M. *et al.*, Estimation of the pseudo homogeneous one dimensional heat transfer coefficient in a fixed bed. *Chem. Engng Process* **20**, 245–253 (1986).
27. Minoura, T., *et al.*, Heat transfer and fluid flow analysis of sinter coolers with consideration of size segregation and initial temperature distribution. *Heat Transfer Jap. Res.* **19**(6), 537–555 (1990).
28. Raju, M. T., *et al.*, Feasibility of a system for sinter cooler waste heat recovery. *Proc. 3rd Int. Symp. on Agglomeration*, Bhubaneswer, 16–18 September 1991, pp. 271–272.
29. Tanaka, N., Waste heat recovery from sintering plants. *Trans. Iron and Steel Inst. of Japan* **20**(3), pp. 200–203 (1980).
30. Reiter, L., Studies on optimizing of waste heat recovery and waste gas recycling on sinter plants. *Proc. 5th Int. Symp. on Agglomeration*, Brighton, 25–27 September 1989, pp. 83–93.
31. Dawson, P. R., Recent developments in iron ore sintering. *Ironmaking Steelmaking* **20**(2), 150–159 (1993).
32. Shirai, T., *Fluidization*, p. 43. Kagakugijutsusha, Tokyo (1958).
33. Hegggs, P. J., Fixed beds. *Heat Exchanger Design Handbook*, Vol. 2, Sec. 2.5, pp. 1–5 (1983).